Annals of Science and Inquiry
Vol. 2 No. 11 (2026)

Two Measurement Channels Give Different Times for a Charging Transition

Kelly Knight · Pamela Dawson · Jack R. Watson

Published: November 26, 2026 | Article 1129

Abstract

A charging power change can appear on different samples in a grid meter and a connector trace. In 17 published laboratory records of unidirectional CCS charging, 378 of 608 logged power-setting changes produced a measurable midpoint on both channels. The connector's DC output reached its midpoint earlier in 192 pairs, on the same sample in 140, and later in 46. The median paired difference was −0.50 seconds, close to the merged records' sampling interval. When each test record carried equal weight, the median of record-level differences was zero. Whether a signal shows a usable transition, and which channel appears to lead, depends on the observation and aggregation rules.

Two Measurement Channels Give Different Times for a Charging Transition

Abstract

A charging power change can appear on different samples in a grid meter and a connector trace. In 17 published laboratory records of unidirectional CCS charging, 378 of 608 logged power-setting changes produced a measurable midpoint on both channels. The connector's DC output reached its midpoint earlier in 192 pairs, on the same sample in 140, and later in 46. The median paired difference was −0.50 seconds, close to the merged records' sampling interval. When each test record carried equal weight, the median of record-level differences was zero. Whether a signal shows a usable transition, and which channel appears to lead, depends on the observation and aggregation rules.

A change in power has several observable timestamps

A power-setting change may be timestamped when it first appears in charger telemetry. The following response can then be recorded by a grid-side analyzer and by the charger at its vehicle-facing output. These measurements may be collected at different instants even when an exported file aligns them to a common time base. If each one is used to mark an event, the resulting timeline can vary. A comparison of the observed times is useful for assessing what the record can resolve before interpreting the order of equipment behavior.

Xu et al. (2026) discuss layered diagnostics and recovery during high-voltage charging across interoperating systems. One requirement for interpreting observations from multiple layers is knowing where the signals originate and what their timestamps represent. The present analysis compares locations in the measurement chain. It estimates the difference between when an observed power change reaches a common fraction on each of two recorded channels. The study does not evaluate an operational fault or a recovery policy. It treats timing as a property of the archived measurements.

Grid demonstrations and charging studies use clocks for different parts of a power response. Wong et al. (2024) evaluate vehicle response capability for grid use, and Striani et al. (2024) report timing and accuracy in an experimental distributed architecture. Pedersen et al. (2025) compare response dynamics for chargers using different interfaces. Dávila-Sacoto et al. (2025) examine implications of response latency in grid studies. These examples make elapsed time a measurable quantity with an application-specific reference. Our question is narrower. Given a common logged setting change in a laboratory trace, do the grid analyzer and DC output channels point to the same transition time?

Selecting recorded changes on a shared laboratory platform

The data are Version 2.0.0 of the TU Dortmund public charging archive from Esser et al. (2024), distributed through Zenodo. The corresponding data descriptor by Esser et al. (2025) documents static and dynamic tests, measurement sources and merging conventions. We join the measurement index to the synchronized export by its published measurement name, retain entries labeled unidirectional dynamic loading and CCS direct current, and use all 17 such entries present in the merged archive. These comprise four Fiat 500e traces, two Honda-e traces, five Opel Corsa-e traces, three Tesla Model Y traces, and three VW ID.4 traces. They were recorded on the EVTEC platform. The changes range from 1 to 12 kW in absolute setpoint increment. This is a low-power laboratory measurement comparison on DC-capable equipment. The setpoint values do not establish a station's rating or describe high-power field operation.

Three synchronized columns define the comparison. AC_Power_set_ID2 is the CCS grid-side setting recorded by the charger. P_kocos_200 is the grid active power from a separate power quality analyzer on the EVTEC system. Output_Power_ID2 is the CCS output power reported in charger telemetry. All three are in kilowatts. The epoch coordinate is used in the exported form without time interpolation. The three columns have separate meanings. The power analyzer and output telemetry represent different measurement points, and the recorded setting is neither of those measurements. Apostolaki-Iosifidou et al. (2017) distinguish input and output measurements when assessing charging losses. We use the distinct signals to compare timestamps on matched reported changes.

The data descriptor explains that the logs are collected with a common time-reference service and that the merged files synchronize measurements originating in distinct records. We retain the synchronized export and its original merged sample coordinates. In these 17 exports, 103,873 complete rows supply the timestamp, setting and both power values. Their per-trace median sample intervals span 0.500 to 0.511 seconds. A reported difference of around half a second is therefore often one row in this representation. There are no cross-channel clock calibrations within this analysis. Ziyat et al. (2023) use high-resolution measurements for charging profiles and electrical waveforms. Yasko et al. (2025) describe a different second-resolution vehicle-side archive. The measurement resolution and sensor placement in both illustrate why timestamps should be interpreted in the frame of the available instrumentation.

A candidate change is a difference of at least 1 kW between consecutive samples of the recorded setting, with direction determined by the sign of that difference. The first changed row supplies time zero. Our calculation of the observed response uses the median power from 12 to four seconds before this row and from 25 to 35 seconds after it, separately on each channel. We require support for the two windows and verify that the setting remains in the expected local state before and after the change. A threshold at half of the difference between the two medians is defined separately for each signal. Changes whose observed median difference in the expected direction is smaller than 0.35 kW do not receive a midpoint. This criterion keeps small changes in nearly flat traces from becoming measured responses simply because they cross a fraction of a very small difference.

The midpoint is the first sampled value on the appropriate side of the threshold in a run of at least three consecutive samples, within the search window from three seconds before to 20 seconds after the logged setting row. The preceding part of the window prevents the analysis from assuming that all linked channels start changing after the logged marker. The following part excludes crossings too far from the selected event. A paired event requires a measurable midpoint on both signals. The paired difference is the CCS output timestamp minus the grid analyzer timestamp. A negative value puts the output first on the merged time grid. We repeat the calculations for a threshold at 90% of each signal's local change. Neither fractional marker estimates the precise physical start of a transient.

Rather than infer independent repeat measurements from many changes on the same trace, we flag the trace as the unit enclosing each repeated test. Bland and Altman (2007) describe why repeated observations from the same unit require careful agreement summaries. We report pooled event counts and a sensitivity taking the median difference within each trace before summarizing across traces. Hyndman and Fan (1996) describe how sample quantiles vary by convention. We use linear interpolation. The associated time offsets describe available pairs after the visibility rule. Counts for unpaired events remain in the results rather than disappearing from the denominator.

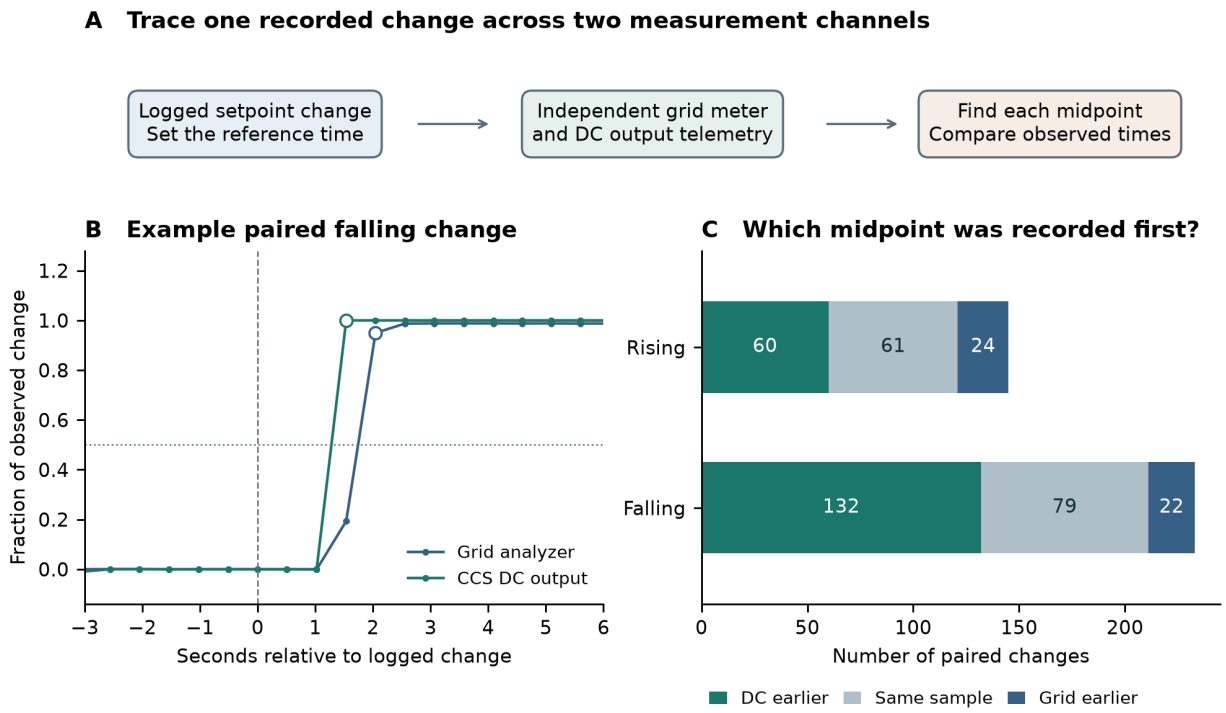

Figure 1. *The logged setting supplies the reference time. Each observed power signal is normalized to its own before-to-after change. Panel B shows a measured falling event in which the DC output midpoint appears at 1.54 seconds and the grid analyzer midpoint at 2.04 seconds. Open markers identify the first samples in the sustained qualifying runs. Panel C counts the ordering of paired midpoints.*

Response coverage and paired timing

The 17 traces contain 608 candidate setting changes, with 304 rising and 304 falling. Both channels pass the primary midpoint rule for 378 changes (62.2%). The other 230 do not yield a pair. In 148 cases both recorded changes fall below the expected-direction amplitude floor. In 69 cases both channels have measurable median changes but lack a sustained midpoint in the shorter search window. The remaining 13 are combinations of a low change or missing crossing affecting individual channels. Differences in measurable coverage matter before the elapsed times are interpreted. A command row and a clearly measurable response under these definitions are separate conditions.

Table 1. Paired midpoint ordering and time differences by recorded setting change.

Analysis group	Candidate changes	Paired changes	DC earlier	Same sample	Grid earlier	Median DC minus grid (s)
All changes	608	378	192	140	46	−0.50
Rising changes	304	145	60	61	24	0.00
Falling changes	304	233	132	79	22	−0.50
Changes of 1 kW	404	273	149	91	33	−0.50
Changes greater than 1 kW	204	105	43	49	13	0.00

The median paired difference is −0.50 seconds, with the middle half spanning −0.51 to 0 seconds. Grid and DC medians measured separately against the setting are 1.52 and 1.50 seconds. The difference of those medians is only about −0.02 seconds. It answers a different statistical question from the median of differences between two observations paired on the same event. The paired statistic accounts for the

association caused by the common change. Most differences are close in magnitude to the approximately half-second sample interval. Forty-six of 378 pairs (12.2%) differ by more than one second in either direction.

Timing coverage differs by direction. The falling changes have 233 pairs (76.6% of candidates) and the rising changes have 145 pairs (47.7%). A DC-first order occurs in 132 falling and 60 rising pairs. The paired subset looks different from the candidate set, which has equal numbers in the two directions. Thus the pooled ordering also reflects the unequal availability of measurable pairs. A setting change with neither midpoint remains a countable case in the coverage assessment. It has no recorded pair from which to infer the relative time.

At the 90% marker, 376 pairs are measured. The paired median is −0.25 seconds, and more than one second separates the marks in 46 cases. These figures show robustness of some counts and a change in the central time difference when the marker changes. If each trace carries equal weight, the median of the 17 within-trace median midpoint differences is zero at the 50% marker. The within-trace medians range from −1.54 seconds to zero. Candidate coverage is especially uneven across vehicle configurations, so a pooled number emphasizes traces contributing more visible changes. The equally weighted check makes that dependence explicit without treating the configurations as independent draws from vehicle fleets.

We examined how the reported ordering responds to changes in the visibility rules that define a pair. Requiring at least 0.50 kW of change instead of 0.35 kW leaves 372 pairs. Keeping the original amplitude floor but ending the crossing search at 15 seconds leaves 374 pairs. In both runs the median paired difference remains −0.50 seconds and 46 pairs still differ by more than one second. Those comparisons show how the central time difference behaves under those two modest changes to the measurement rules. The fraction used to mark the transition itself has a larger effect on the median than these changes in which candidate windows qualify.

The observed tail is asymmetric. The CCS output is at most 1.02 seconds later than the grid analyzer under the primary rule, while the largest lead is 8.65 seconds. In the latter recorded change, the DC midpoint occurs approximately 0.51 seconds after the first changed setting row, and the grid midpoint at about 9.16 seconds. The result concerns this record's crossing times under the specified reference windows. A difference in trajectory shape through a window can move its midpoint even if the transition has already begun. These data leave the physical reason for the longer crossing interval unresolved.

Interpreting an observed lead at two measurement points

A channel closer to the vehicle and a channel closer to the supply can exhibit different shapes through a transition. The position of the midpoint depends on both the recorded shape and the before-and-after reference. Rauma et al. (2021) describe nonidealities in charging management. Modeling work by Chen and Rincon-Mora (2006) and Hu et al. (2012) gives context for dynamic electrical responses. Meng et al. (2015) and Mousavizade et al. (2025) examine broader grid-response questions. Our paired counts lack the synchronized physical evidence needed to allocate a measured lag to a specific internal process. They demonstrate how the observed ordering changes with the channel and event definition.

Recording both midpoints with their observation interval preserves details that an ordered list would discard. A same-sample result says the two markers occupy one stored row. It leaves their ordering within that interval open. A result split across adjacent rows can reflect a short separation in the sources or measurement and alignment conventions. Neither observation determines the precision with which an unrecorded internal event can be timed. If the underlying research question requires assigning a cause or a specific time to a change inside the equipment, the comparison would need a reference clock tied to each

relevant measurement and a separately characterized acquisition delay. The public archive supports an observational audit without those additions.

Fast-charging profile research at other scales has different timing objectives. Li et al. (2025) model the shape and duration of field charging, and Simolin et al. (2025) examine profile heterogeneity. Thurston and Wells (2023) describe high-power profile characterization. Borlaug et al. (2023) and Lappalainen and Kleissl (2023) use charging records for utilization or design questions. Those outputs are interpretable through their own measurement boundaries. The synchronized lab comparisons here are about event markers within records, under moderate power changes. They supply no direct estimate of a comparable difference near the rated output of a public high-power station.

The same limitation applies to reliability. Watt et al. (2025) examine initialization timings with measures of different stages, and Quinn et al. (2024) define customer-focused performance indicators. Rempel et al. (2024), Gamage et al. (2024), and Yu et al. (2025) use field evidence to study reliability, access or station performance. An analyst using disagreements between timing records would need related status and timestamp evidence before representing them as exceptions in such indicators. The present measurement comparison indicates that the chosen signal and marker are relevant even when there is one logged setting event. It does not support counting an extra delay as a charging failure.

Reproduction and observation scope

The selected members were obtained from pinned public byte ranges and checked against published ZIP member metadata. The study files record the member checksums and the timing output for each setting change. Source trace, instrument label, row coverage, and event direction remain available for inspecting how pooled values were produced. This provenance follows the reuse and documentation principles articulated by Wilkinson et al. (2016) and Gebru et al. (2021), and the executable analysis approach discussed by Peng (2011).

The central timing difference is small in relation to the available sampling interval, yet the ordering of measurements is often nonidentical across channels. A logged timestamp for a power transition is meaningful when the observation site, threshold definition, and synchronization context travel with it. Such a record can be compared across studies while keeping measured timing distinct from any inference about physical or operational cause.

References

Apostolaki-Iosifidou, Elpiniki; Codani, Paul; Kempton, Willett (2017). Measurement of power loss during electric vehicle charging and discharging. *Energy, 127, 730–742*. DOI.

Bland, J. Martin; Altman, Douglas G. (2007). Agreement Between Methods of Measurement with Multiple Observations Per Individual. *Journal of Biopharmaceutical Statistics, 17(4), 571–582*. DOI.

Borlaug, Brennan; Yang, Fan; Pritchard, Ewan; Wood, Eric; Gonder, Jeff (2023). Public electric vehicle charging station utilization in the United States. *Transportation Research Part D: Transport and Environment, 114, 103564*. DOI.

Chen, Min; Rincon-Mora, G.A. (2006). Accurate electrical battery model capable of predicting runtime and I-V performance. *IEEE Transactions on Energy Conversion, 21(2), 504–511*. DOI.

Dávila-Sacoto, Miguel; González, Luis Gerardo; Zorita-Lamadrid, Ángel Luis; Espinoza, Juan Leonardo (2025). Effect of latency and charge control of electric vehicles in power grids with high penetration of photovoltaic solar energy. *Renewable Energies, 3(1), 27533735251342114*. DOI.

Esser, Marcel; Spina, Alfio; Rehtanz, Christian (2024). Bidirectional and Unidirectional Charging Profiles of Electric Vehicles. *Zenodo, Version 2.0.0*. DOI.

Esser, Marcel; Orfanoudakis, Stavros; Homaee, Omid; Vahidinasab, Vahid; Vergara, Pedro P.; Spina, Alfio (2025). High-temporal-resolution dataset of uni-, bidirectional, and dynamic electric vehicle charging profiles. *Scientific Data, 12(1), 1192*. DOI.

Gamage, Tisura D.; Jenn, Alan T.; Tal, Gil (2024). Novel Methodology to Measure the Reliability of Public DC Fast Charging Stations. *Transportation Research Record: Journal of the Transportation Research Board, 2678(11), 1440–1453*. DOI.

Gebru, Timnit; Morgenstern, Jamie; Vecchione, Briana; Vaughan, Jennifer Wortman; Wallach, Hanna; III, Hal Daumé; Crawford, Kate (2021). Datasheets for datasets. *Communications of the ACM, 64(12), 86–92*. DOI.

Hu, Xiaosong; Li, Shengbo; Peng, Huei (2012). A comparative study of equivalent circuit models for Li-ion batteries. *Journal of Power Sources, 198, 359–367*. DOI.

Hyndman, Rob J.; Fan, Yanan (1996). Sample Quantiles in Statistical Packages. *The American Statistician, 50(4), 361–365*. DOI.

Lappalainen, Kari; Kleissl, Jan (2023). Sizing of stationary energy storage systems for electric vehicle charging plazas. *Applied Energy, 347, 121496*. DOI.

Li, Siyi; Zhang, Mingrui; Doel, Robert; Ross, Benjamin; Piggott, Matthew D. (2025). Deep learning predicts real-world electric vehicle direct current charging profiles and durations. *Nature Communications, 16(1), 10921*. DOI.

Meng, Jian; MU, Yunfei; WU, Jianzhong; JIA, Hongjie; DAI, Qian; YU, Xiaodan (2015). Dynamic frequency response from electric vehicles in the Great Britain power system. *Journal of Modern Power Systems and Clean Energy, 3(2), 203–211*. DOI.

Mousavizade, Mirsaeed; Garmabdari, Rasoul; Bai, Feifei; Taghizadeh, Foad; Sanjari, Mohammad J.; Alahyari, Arman; Hossain, Md. Alamgir; Mahmoudian, Ali; Lu, Junwei (2025). A Bayesian approach to modeling fast chargers functionality for grid frequency support. *Applied Energy, 384, 125452*. DOI.

Pedersen, Kristoffer Laust; Knudsen, Rasmus Meier; Marinelli, Mattia; Secchi, Mattia; Sevdari, Kristian (2025). Enabling Grid Services with Bidirectional EV Chargers: A Comparative Analysis of CCS2 and CHAdeMO Response Dynamics. *World Electric Vehicle Journal, 16(11), 636*. DOI.

Peng, Roger D. (2011). Reproducible Research in Computational Science. *Science, 334(6060), 1226–1227*. DOI.

Quinn, Casey W.; Cardinali, Sarah; Clifford, Jason; Houck, Kaleb; Moriarty, Kristi; Savargaonkar, Mayuresh; Smart, John G.; Smith, David E.; Varghese, Benny J. (2024). Customer-Focused Key Performance Indicators for Electric Vehicle Charging. *Idaho National Laboratory*. DOI.

Rauma, Kalle; Simolin, Toni; Rautiainen, Antti; Järventausta, Pertti; Rehtanz, Christian (2021). Overcoming non-idealities in electric vehicle charging management. *IET Electrical Systems in Transportation, 11(4), 310–321*. DOI.

Rempel, David; Cullen, Carleen; Matteson Bryan, Mary; Vianna Cezar, Gustavo (2024). Reliability of Open Public Electric Vehicle Direct Current Fast Chargers. *Human Factors: The Journal of the Human Factors and Ergonomics Society, 66(11), 2528–2538*. DOI.

Simolin, Toni; Järventausta, Pertti; Paolone, Mario (2025). Analysis and modelling of DC fast-charging profiles of heterogeneous EVs. *Transportation Engineering, 20, 100350*. DOI.

Striani, Simone; Pedersen, Kristoffer Laust; Engelhardt, Jan; Marinelli, Mattia (2024). Experimental Investigation of a Distributed Architecture for EV Chargers Performing Frequency Control. *World Electric Vehicle Journal, 15(8), 361*. DOI.

Xu, Dan; Gui, Hao; Chen, Huangyin (2026). Research on Layered Control and Fault Recovery Mechanisms for Fast Charging Safety Diagnosis of High-Voltage Battery Systems Under Charging Network Interoperability Conditions. *2026 3rd International Conference on Electrical Technology and Automation Engineering (ETAE), 669–672*. DOI.

Thurston, Sam; Wells, Landon (2023). EVs@Scale Next-Gen Profiles – EV Profile Capture 2023. *Argonne National Laboratory*. Source.

Watt, Ed; Bani Shamseh, Mohammad; Gadamsetty, Pranav (2025). Quantifying Time to Charge. *ChargeX Consortium, U.S. Department of Energy*. Source.

Wilkinson, Mark D.; Dumontier, Michel; Aalbersberg, IJsbrand Jan; Appleton, Gabrielle; Axton, Myles; Baak, Arie; Blomberg, Niklas; Boiten, Jan-Willem; da Silva Santos, Luiz Bonino; Bourne, Philip E.; Bouwman, Jildau; Brookes, Anthony J.; Clark, Tim; Crosas, Mercè; Dillo, Ingrid; Dumon, Olivier; Edmunds, Scott; Evelo, Chris T.; Finkers, Richard; Gonzalez-Beltran, Alejandra; Gray, Alasdair J.G.; Groth, Paul; Goble, Carole; Grethe, Jeffrey S.; Heringa, Jaap; 't Hoen, Peter A.C; Hooft, Rob; Kuhn, Tobias; Kok, Ruben; Kok, Joost; Lusher, Scott J.; Martone, Maryann E.; Mons, Albert; Packer, Abel L.; Persson, Bengt; Rocca-Serra, Philippe; Roos, Marco; van Schaik, Rene; Sansone, Susanna-Assunta; Schultes, Erik; Sengstag, Thierry; Slater, Ted; Strawn, George; Swertz, Morris A.; Thompson, Mark; van der Lei, Johan; van Mulligen, Erik; Velterop, Jan; Waagmeester, Andra; Wittenburg, Peter; Wolstencroft, Katherine; Zhao, Jun; Mons, Barend (2016). The FAIR Guiding Principles for scientific data management and stewardship. *Scientific Data, 3(1), 160018*. DOI.

Wong, Shen Yuong; Liang, Kaihan; Goh, Hui Hwang (2024). Evaluation of electric vehicle response capability in power grid. *MethodsX, 12, 102783*. DOI.

Yasko, Mohamed; Moussa Issaka, Adamou; Tian, Fanghao; Kazmi, Hussain; Driesen, Johan; Martinez, Wilmar (2025). Unveiling Energy Dynamics of Battery Electric Vehicle Using High-Resolution Data. *Scientific Data, 12(1), 1878*. DOI.

Yu, Qiao; Que, Tristan; Cushing, Lara J.; Pierce, Gregory; Shen, Ke; Kejriwal, Mayank; Yao, Yuan; Zhu, Yifang (2025). Equity and reliability of public electric vehicle charging stations in the United States. *Nature Communications, 16(1), 5291*. DOI.

Ziyat, Isla; Gola, Alia; Palmer, Patrick R.; Makonin, Stephen; Popowich, Fred (2023). EV Charging Profiles and Waveforms Dataset (EV-CPW) and Associated Power Quality Analysis. *IEEE Access, 11, 138445–138456*. DOI.